Egypt. J. Phys. **Vol. 45,** pp. 49 - 57 (2017)

Effect of ZnO and Al_2O_3 Addition on the Physical Properties of Cobalt Doped Phosphate Glass

N.H. Moussa
Physics Department, Faculty of Science, Al-Azhar University, Cairo, Egypt

GLASS system of chemical composition 49.5 P_2O_5– (30-X) ZnO–XAl_3O_2 -20Na_2O-0.5 CoO with (X= 0, 2,5,7.5 and 10 mole%) hase been prepared by melt quenching technique. The amorphous nature was confirmed by X-ray diffraction (XRD).

The density has been measured using Archimedes method the density (ρ) and molar volume M_v follow apposite trend. The density decreases (ρ) while molar volume (Mv) increase with increasing Al content. This is most likely due to the difference in molecular weights of ZnO and Al_2O_3.

Using optical absorption, the optical band gap energy has been determined and was found to decrease with increasing Al_2O_3 content on the other hand Urbach energy (ΔE) increases, by increasing Al_2O_3.

Cobalt behave as band pass filters. The characterized parameters of these filters.i.e. area, center, width and height of band pass, have been estimated. The crystal field (D_q) and the Racah parameters (B) were evaluated.

Introduction

Oxide glasses find enhanced interest dueto their peculiar properties and wide range of applications. However, phosphate glasses exhibit special properties such as lower thermal conductivity mechanical strength, and higher thermal expansion coefficient [1-9]. Incorporation of aluminum into phosphate glasses can modify optical, electrical and magnetic properties that make them suitable for different applications such as superionic conductivity [10-12]. Sodium phosphate glasses dapped by transition metal are very important in photonic and biological application [13-15] also acts as a good modifier whichis usually added to improve the chemical durability.

Glasses dapped with transition metal ions have attracted a great deal of attention because of the capability of the ions to exist in more than one valence state enabling electrical conduction to occur by hopping of carriers from lower to higher valence state [16]. In glasses, cobalt ions can exhibit divalent or trivalent states (*i.e.* CO^{2+}, CO^{3+}). Under tetrahedral symmetry, the CO^{2+} ions exhibit strong colorant features, which produces an intense blue color, while a pink color is produced for octahedral symmetry [17, 18-20].

Therefore, the glass color strongly depend on the latter, and ligand field parameters [21,22]. The electronic configuration of Co^{2+} (d^7) in octahedral coordination it exhibits three absorption bands associated with the spin-allowed transition from $^4T_1(F) \rightarrow {}^4T_2(H)$, $^4T_1(^4F) \rightarrow {}^4A_2(^4F)$ and $^4T_1(^4F_1) \rightarrow {}^4T_1(^4P)$ likewise, Co^{2+} in tetrahedral symmetry exhibits two transitions from $^4A_2(^4F) \rightarrow {}^4T_1(^4P)$ and $^4A_2(^4F) \rightarrow {}^4T_1(^4F)$ [23, 24]

Experimental Methods

Glass system of chemical composition 49.5 P_2O_5–(30-X) ZnO – XAl_2O_3 – 20Na_2O – 0.5 CoO where (X = 0, 2.5, 5, 7.5, 10 at %) was prepared using the melt quenching technique.

The chemical composition of the investigated five systems is shown in Table 1.

The corresponding weights of each sample were mixed and grinded using morter for 20 min. Hence, the samples in open porcelain crucible and calcined at 340°C for 1 hr to release underside gases. The furnace was then raised 950°C for 30 min.

TABLE 1.

Ratio					Al_2O_3	ZnO	P_2O_5	Na_2O	CoO	800
Al_2O_3Mol(%)	ZnOMol(%)	P_2O_5Mol(%)	Na_2O Mol(%)	CoOMol(%)	0.12745	0.101725	0.33015	0.132488	0.09366574	Sum
0	30	49.5	20	0.5	0.0000	3.0518	16.3424	2.6498	0.0468	22.043925
2.5	27.5	49.5	20	0.5	0.3186	2.7974	16.3424	2.6498	0.0468	22.108238
5	25	49.5	20	0.5	0.6373	2.5431	16.3424	2.6498	0.0468	22.17255
7.5	22.5	49.5	20	0.5	0.9559	2.2888	16.3424	2.6498	0.0468	22.236863
10	20	49.5	20	0.5	1.2745	2.0345	16.3424	2.6498	0.0468	22.301175

The prepared samples were immediately transferred into preheated stainless steel molds for annealing adjusted at 340°C to remove internal stress. The melts samples were quenched in between two brass plates to produce disc of about 0.2 cm thickness. The samples exhibit a clear pink color. X-ray diffraction (XRD) spectra were obtained on (a shimadzu XD3A) diffractometer. Glass densities were measured by using the Archimedes's method with toluene as an immersion solvent. The optical absorption spectra of glass samples were taken at room temperature on (Jasco V670) spectrophotometer in the region (190-1100 nm).

Results and Discussion

X-ray diffraction

The amorphous nature of the glass samples was confirmed by the X-ray diffraction (XRD) (Fig. 1). The (XRD) pattern of the glass samples shows no sharp peaks, indicting the non crystalline nature of the prepared samples.

Physical properties

The density (ρ) measurement has a vital role for the prediction of the structure change caused in the glass network by the replacement of oxides.

The densities of the inspected samples were calculated according to Archimedes method using toluene, as an immersion liquid(ρo=0.8669g/cm^3) by the following relation.

$$\rho = \frac{W_{air}}{W_{air} - W_1}\rho$$

whereW_{air} and W1 are the weight of the sample in air and toluene, respectively. The molar volume (M_v) can be calculated in terms of the density (ρ) of glass and its molar mass (M) by

$$M_{v} = \frac{M}{\rho}$$

The density (ρ) and calculated molar volume (Mv) of glass samples are plotted as a function of glass samples are plotted as a function of Al2O3 content as shown in Fig. 2 and Fig. 3 respectively and tabulated in Table 2.

It is found that the density (ρ) and molar volume Mv followed an opposite trend, *i.e.* it follows the normal behavior [23-24]. The replacement of light Zn content by heavier Al content is responsible for the decreasing density from 3.5 to 3.31 then it

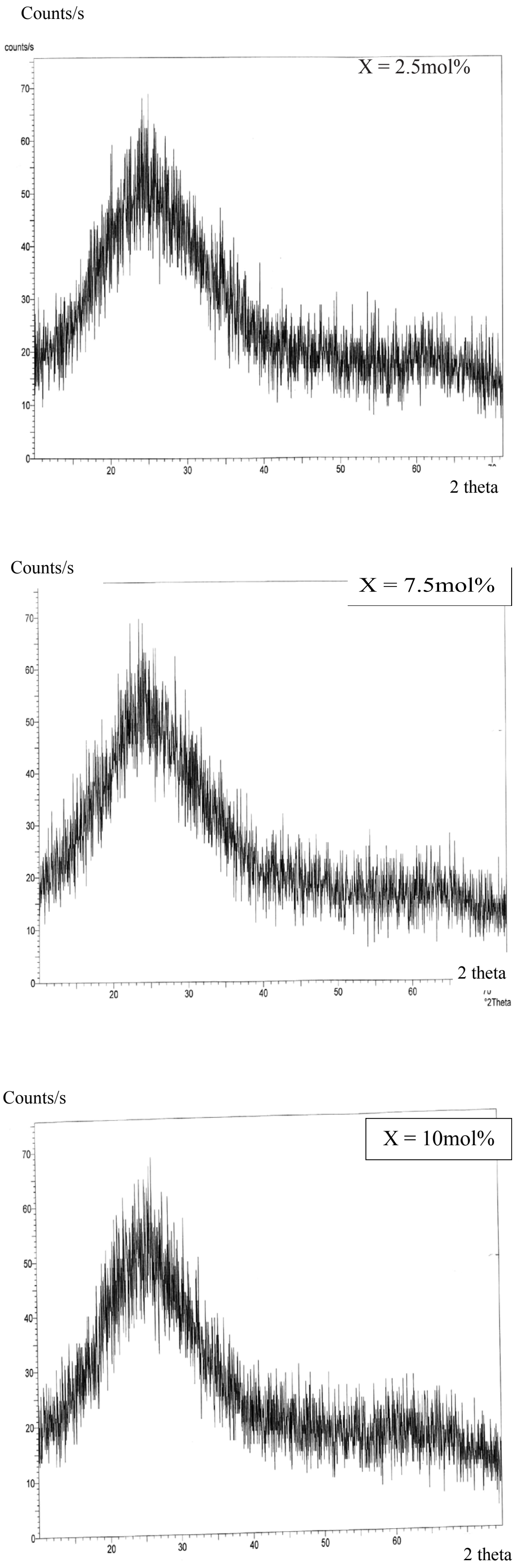

Fig. 1. The (XRD) pattern of the glass samples.

starts to increase up to 7.5 this is most likely due to the difference in molecular weights of ZnO and Al_2O_3 beside the role of additive of oxide former or modifier. is given by [27]:

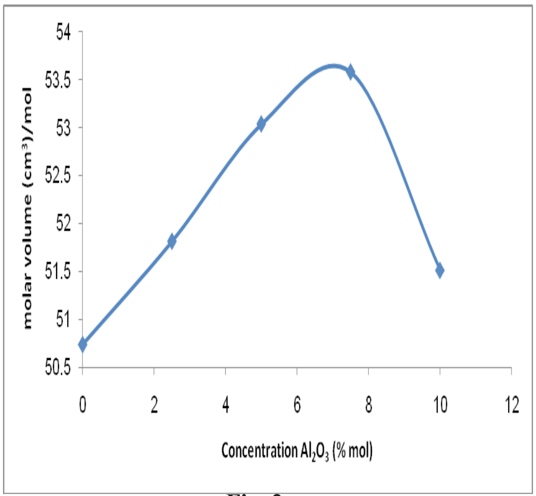

Fig. 2.

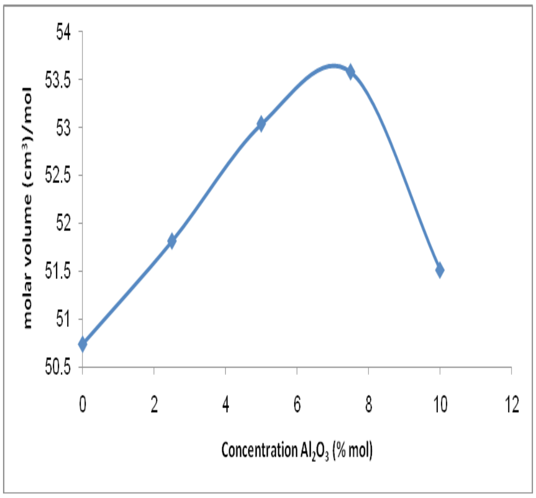

Fig.3.

TABLE 2. The density (p) and molar volume (M_v) of the sample glasses

Concentration Mol (%)	r(m/cm³)	M_v (cm³/mole)
0%	3.50	50.7
2.5%	3.42	51.8
5%	3.35	53.03
7.5%	3.31	53.58
10%	3.45	51.51

Optical band gap energy (E_{opt}) and Urbach energy (ΔE)

The optical absorption spectroscopy is a useful technique to understand the electronic band structure in glasses. The absorption spectra of glass samples at room temperature shown in Fig. 4 which were recorded in the wave length range (190-1100 nm).

The optical absorption may be displaced in a number of ways as a function of photon energy (hυ). In the following equation (1) [25]. The absorption coefficient (α) of the glass systems was calculated.

$$\alpha(\upsilon) = \frac{1}{t} \log \frac{I_o}{I} = 2.303 \frac{A}{d} \qquad (1)$$

Where (I_o) and (I) are the intensities of incident and transmitted light, respectively, (A) is the absorbance for each sample and (t) is the sample thickness.α(υ) can be related to optical band gaps for direct and indirect transitions according to the following equation [26].

$$\alpha(\upsilon) = B \, \underline{(hv - E_{opt}} \qquad (2)$$

where B is the constant, $E_{opt}$is the optical band gap energy, and n may have the following values (2),(3), (1/2) and (1/3) depending on interband electronic transition direct or indirect. The data reveals that in the present case (n=2), indicating an indirect transition. In order for calculating the optical band gap, the amount of $(\alpha h\upsilon)^{1/2}$ is plotted versus the energy of light (hυ) for all samples.

(E_{opt}) values can be obtained by extrapolation of linear region of the plots to the (hυ) axis for indirect transition, as shown in Fig. 5.

The optical band gap energy (E_{opt}) is a function of Al content as shown in Fig. 6.

The optical band gap energy decreased from 5.5 to 5.1 by increasing X = 0 to (X = 5) then it started increasing at (X = 7.5) the tail–width of the absorption spectra can also be used to analyze possible changes in the glass structure [26]. The tail – width exhibited an exponential increase and

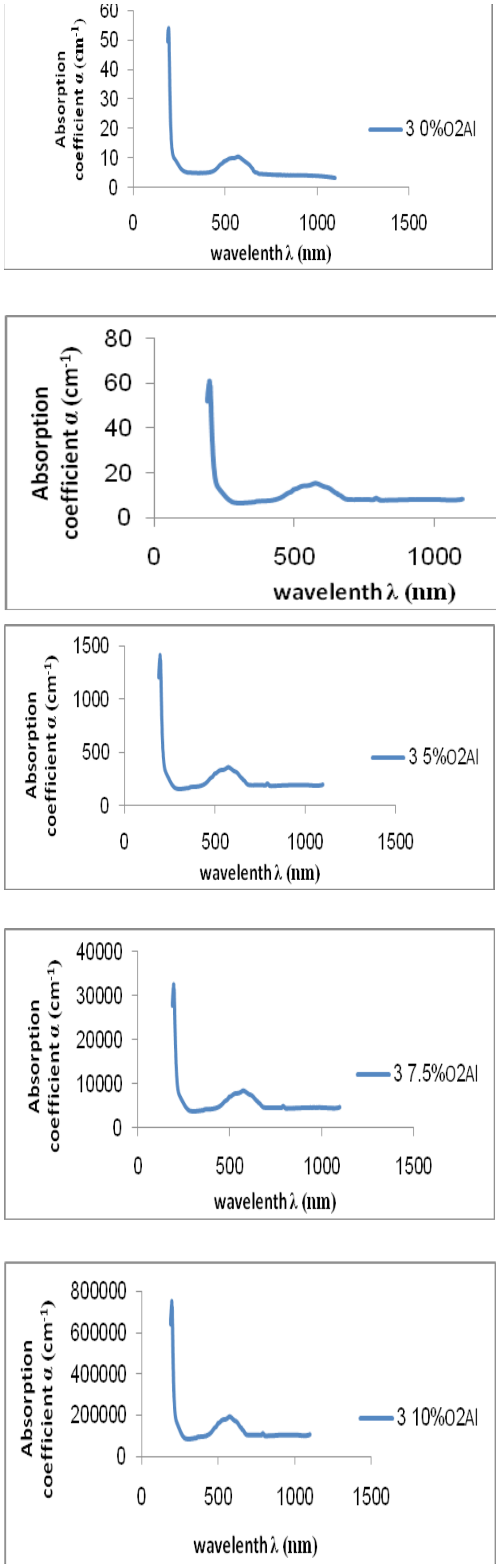

Fig. 4. Optical absorption spectra for the glass samples of 0.2 cm thickness.

$$\alpha(\upsilon) = \alpha_o \, exp^{\left(\frac{h\upsilon}{\Delta E}\right)} \quad (3)$$

where (α_o) is a constant, (hυ) is the photon energy and (ΔE) is the Urbach energy which indicates the width of the band tail of the localized states in the band gap. The Urbach energy (ΔE) values of the investigated samples were determined by taking the reciprocals of the slopes of the linear portion of the ln(α) versus (hυ) plots as shown in Fig. 7.

The obtained values of (E_{opt})and (ΔE) are listed in Table 3 indicated that (ΔE) decreases with in increasing Al content while the optical energy gap decreases. The band tail width was estimated and shown as a function of Al content as shown in Fig. 8.

It is clear that the band tail width follows opposite trend to that of energy gap observed beheavior of both (E_{opt}) and (ΔE) allows to conclude that the electron transition takes place across the mobility gap.

Cobalt optical absorption

The transition metals are characterized by incomplete (3d) shell which results in inter band transition between (3d) sublevels. Such transitions are usually forbeddin due to selection roles. However, it take place due to the relation of selection rules. Such transitions lay in the visible region which give transition metal compounds a given colour. In glasses cobalt ions can acted upon by octahedral or tetrahedral ligand field. The latter leads to splitting of (3d) energy levels giving rise to absorption bands allowing determination of ligand field and some information about the degree of covlency of their bonds. The pink colour of prepared glasses and optical absorption reveal that the Co ions are acted upon by both octahedron and tetrahedron. Figure 9 shows the optical absorption spectra of Co ions were recorded in the wave length range (400 -700) nm.

The host glass has no absorption bands, however, for samples with Co ions introduced into the glass network. The optical absorption bands were deanvoluted. The deconvalution has been done assuming Gaussion function.The obtained values are listed in Table (4), along with their assailment.

From the estimated positions of the experimentally allowed transition, the parameters such as crystal field parameters (D_q) and the Racah parameter (B) can be calculated from [28-29].

$$B = \frac{1}{510}[7(\upsilon_2 + \upsilon_3) \pm \{49(\upsilon_2 + \upsilon_3)^2 + 680(\upsilon_2 - \upsilon_3)^2\}] \quad (4)$$

$$10D_q = \frac{1}{3}(\upsilon_2 + \upsilon_3) \; - 5B \quad (5)$$

The estimated values of ligand parameters (D_q) and (B) are listed in Table 5.

Conclusion

Glass system composition 49.5 P_2O_5 – (30-X) ZnO-XAl_2O_3 – 20 Na_2O–0.5 CoO. With (X=o, 2.5, 5, 7.5, 10 mol %) has been prepared by melt quenching technique. The amorphous nature is indicated by X-ray diffraction. Several physical parameters, such as density () and molar volume (M_v) were measured.

All measured properties show non linear depend on composition.

Density (ρ) and molar volume (M_v) show opposite trends the observed absorption edge extended over wide range of wave lengths. This agreas with the amorphous nature of glasses. The energy gap was estimated from optical measured data. It is found that (E_g) decrease with increase Al content while as (ΔE) follows opposite trend.

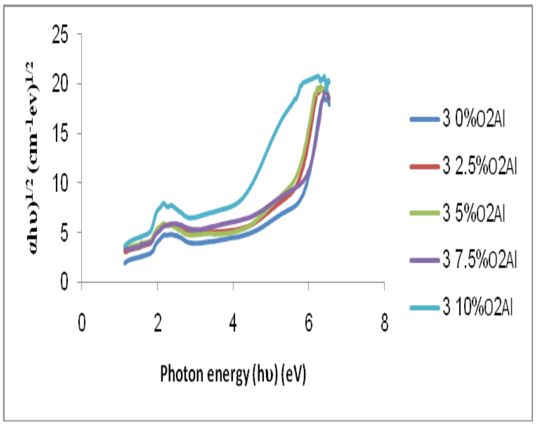

Fig. 5.

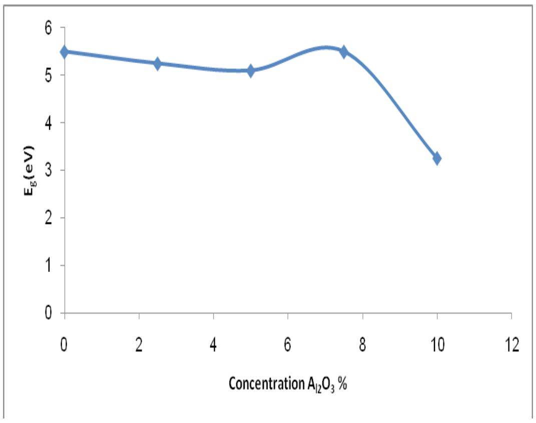

Fig. 6. The variation of Eg of the samples glass for different concentration of Al2O¬3.

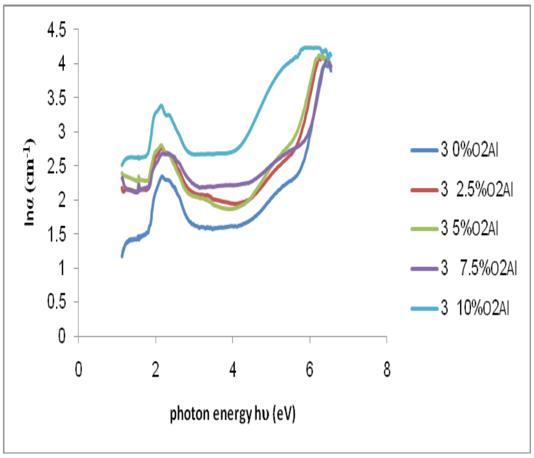

Fig. 7. Urbach plot for the glass samples .

TABLE 3. The concentration of the chemical composition, band tail energy (ΔE) and optical band energy gap (E_{opt}).

Concentration Mol (%)	ΔE(eV)	E_{opt}(eV)
0%	0.71	5.5
2.5%	0.76	2.25
5%	0.90	5.1
7.5%	1.0	5.5
10%	1.81	3.25

TABLE 4. The band position of the glass system of chemical composition.

Conc. (mol%)	Peak	Area	Center	Width	Height
	1	52.402	538.55	141.82	0.29482
0%	2	2.1911	579.70	32.542	0.053722
	3	5.2085	629.07	50.628	0.82085
2.5%	1	34.521	531.29	98.809	0.27876
	2	1.6226	576.72	25.431	0.050909
	3	19.660	617.81	76.433	0.20523
5%	1	21.450	535.26	77.2228	0.22161
	2	2.8127	577.50	27.343	0.082074
	3	21.725	618	69.930	0.24787
7.5%	1	35.253	519.22	109.36	0.25720
	2	10.159	589.93	59.751	0.13566
	3	4.4765	641.20	39.181	0.091161
10%	1	59.392	536.71	93.787	0.50527
	2	7.1022	579.18	29.603	0.19142
	3	32.922	623.36	56.085	0.46837

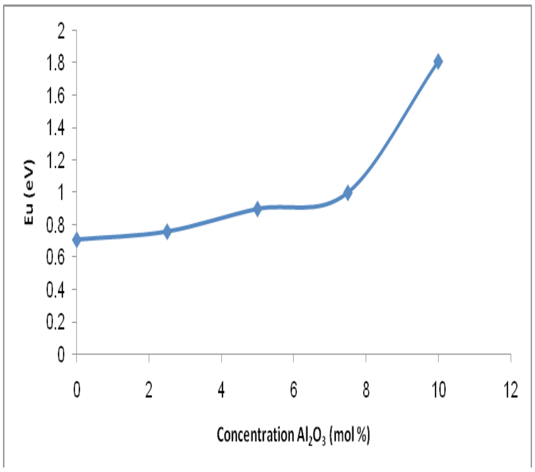

Fig. 8. The variation of Urbach energy of the glass samples with concentration Al2O3

TABLE 5. Optical parameters.

X(mol%)	B(cm^{-1})	Dq(cm^{-1})
0	1501.7	711.9
2.5	1512.5	717.3
5	1507.7	714.9

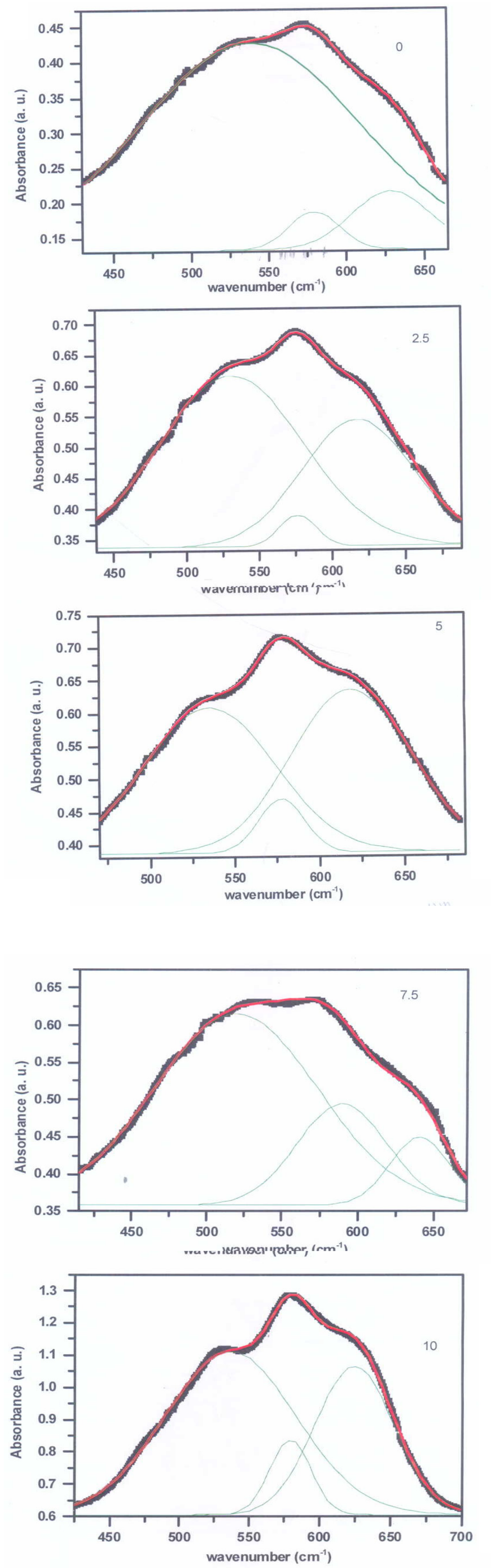

Fig. 9.

References

1. Yang Li, Joanhu Yang, ShiqingXu, Guonian Wang LiLi Hu, Physical and Thermal Properties of P2O5–Al2BaO – LaO3 glass, *J. Matter Sci. Techol.* **21**,391-394(2005).

2. Das, S.S. VibaSrivastava and Singh, P. Ionic transport in sodium phosphate glass doped with chlorides of Co, Cd and Ag Indian *J. Eng. Mater. Sci.* **13**, 455-461 (2006).

3. Elhaes,H., Attallah,M., Elbashar, Y., El-Okr, M. and Ibrahim, M. Application of Cu2¬O – doped phosphate glasses for banpass filter, physica **B449,** 251-254(2014).

4. HananElhaesAttallah,YahiaElbashar, Ayser Al-Alousi, Mohamed El-Okr, Medhat Ibrahim Modeling and optical properties of P2O5- ZnO-CaO Na2O glasses doped with copper oxide, J. computetheor. *Nanosci* **11,** 1-6(2014).

5. PetruPascuta, Gheorghe Borodi, NicolaieJumate., Joan Vida – Simiti, Dan Viorel. EugenCulea, the structural role of manganese ions in some Zinc phosphate glasses and glass ceramics. *J. Alloys compd* **504,** 479-483(2010).

6. Cetinkayacalak,S., Aral Optical, E. and thermal properties of P2O5 – Na2O — Al2O3 – CaO glasses doped with transition metals *J. Alloys copd.* **509,** 4935-4939(2011).

7. Christoph Stahli Maziar Shah Mohammadi,

Kristian E. water Showan N. Nazhat Characterizaion of aqueous interactions of copper – doped phosphate – based glasses by vapour sportion Acta Biomater. **10,** 3317-3326(2014) .

8. A. Chanhine M. Ettabirou , M. Elbenaissi M. Haddad J. L. Pascal Effect of CuO on the structure and properties of (50-X/2) Na2O-xCuo –(50-X/2) Po2O5 glasses mater chem. Phys. **84,** 351-347(2004).

9. El-SayedYoysee A. E. Al-Salami, Mario Hotzel, Optical and Thermal characteristics of glasses based on TeO2 *Bull Mater Sci.* **35,** 96-96(2012).

10. Rayan, D.A. Elbashar, Y.H. Rashad,M.M. and El-Korashy,A. Optical Spectroscopic analysis of cupic oxide doped barium phosphate glass for sand pass absorption filter, *Journal of Non-crystalline solids* **382,** 52-57 (2013)

11. Nehal Aboulfotoh, Yahia Elbashar, Mohamed Ibrahem and Mohamed El-okr, characterization of copper doped phosphate glasses for optical applications, ceramics *International* **40,** 10395-10399(2014)

12. Sulowsha,J. Waclawska,I. and Oleiniczak,Z. structural studies of copper – containing multicomponent glasses from the SiO2–P2O5 – K2O- CaO – MgO system. *Journal of vibrational spectroscopy* **65,** 44-49 (2013).

13. Ali Ersundu, MirayCelikbilek, Mohamed Baazouzi, Mohamed Soltani, JohamTroles, SuheylaAydin. Characterization of new Sb2O3 – based multicomponent heavy metal oxide glasses. *J. Alloys. Compd.* **615,** 712-718 Elsevier (2014)

14. Yahia H. Elbashar Structural and spectroscopic analysis of copper doped P2O5–Zno–K2O–Bi2O3 glasses, Int., *J. Process. Appl. Ceram.* **9**(3) 169-173(2015) .

15. Y.H. Elbashar, Aly Saaed, Computational spectroscopic analysis by using clausisus – Massotti method for sodium borate glassdoped neodymium oxide Res., *J. Pharm. Biol. Chem. Sci* (RJPBCS) **6,**320-326(2015).

16. A.S. Shawoosh, A. A. Kutub, An investigation of the electrical, optical and DSC properties of copper – Phosphate glass composition , *J. Mater, Sci.* **28,** 5060(1994)

17. Marzauk,M.,Abo –Naf, S., Zayed, H.A., Hassan,N.S. *J. Matr Res. Technol.,* **5,** 226-233(2016).

18. Naresh,P., Naga, G., Raju Ch. Srinivasa Rao. S. Prassad Ravibumar,V. Nveeraiah, *Phys.* **B 407** 712-718(2012).

19. Uniyal, A. and Singh, S.P. *J. Pure Appl. Phys.* (109-111)(2004) .

20. (20) G. Laurence, C. Laurent C. Georges, B. Valeric, J. Non – Cryst. Solid 293-295 105-111(2001) .

21. Nagariyima,G.,Satynarayana,A.T.,Gandheb. B.Y. Satyanaryana,P.V.V. and Veeriah, A. N. *Solid State Commun* **150,** 9-13(2010).

22. A. Terczbska – Madej. Kcholewalska, M. *Loczka. Opt. Mater.* **32 ,**1456-1462(2010).

23. Shih, P.Y. and Chin, T.S. *Material Chemistry and Physics* **60**,50-57(1999) .

24. Venkateswara,G., Rao and Beeraiah, V. *J. Alloys compounds* **339,**54-64 (2002) .

25. Davis,E.A. and Matt, N.F., *Philios Mag.* **22,** 903-922(1970) .

26. Mott,N.F. and Davis, E.A., *Philos Mag.* **17** 1269-1284(1968).

27. F. Urbach. *Phys. Rev.* **92,** 1324(1953). (28) F Ahmed, E Hassan Aly. M. Atef , M.M. Elokr, *J. Alloys comp.* **593,** 250-255(2014).

28. Beayry,L., Derouet, J. and Binet,L. *J. Solid State Chem.,* **177,** 1437-1443(2004) .

(Received: 2 / 1/ 2017;
accepted: 18 /7 / 2017)

دراسة الخواص الفيزيائية للنظام الزجاجي بإضافة اكسيد الزنك و اكسيد الالومنيوم و الكوبلت

نعيمة حسين موسى
قسم الفيزياء -كلية العلوم (فرع البنات) جامعة الازهر – مدينة نصر – القاهرة

تم اختيار النظام الزجاجي التالي :

49.5P2O5-(30-X)ZnO – XAL3O2 – 20Na2O - 0.5CoO

Where (X = 0 , 2.5 , 5 , 7.5 and 10 mol%)

وتم تحضير العينات بتقنية التبريد بعد صهر العينات وتم استخدام حيود الاشعة السينية وقد اكدت النتائج الصورة الامورفية (غير المتبللرة) للعينات وتم قياس الكثافة وذلك بطريقة ارشيميدس ومن ثم حساب الحجم المولاري ووجد ان الكثافة تقل بينما الحجم المولاري يزيد بزيادة اكسيد الالومنيوم وهذا ناتج عن الفرق في الوزن الجزيئي لاكسيد الزنك واكسيد الالومنيوم وبدراسة الضوئية للعينات وجد ان energy gap الخواص تقل بزيادة اكسيد الالومنيوم بينماEurbach energy. تزيد بزيادة اكسيد الالومنيوم واستخدم الكوبلت كمرشح ضوئي وقد تم حساب المعاملات الضوئية مثل :

Racah parameter , Crystal field parameter